Enhancing the anti-lymphoma potential of 3,4-methylenedioxymethamphetamine ('ecstasy') through iterative chemical redesign: mechanisms and pathways to cell death

Wasik, AM; Gandy, MN; McIldowie, M; Holder, Michelle; Chamba, Anita; Challa, Anita; Lewis, KD; Young, Stephen; Scheel-Toellner, Dagmar; Dyer, MJ; Gordon, John; Barnes, Nicholas; Piggott, MJ

DOI:
10.1007/s10637-011-9730-5

Document Version
Peer reviewed version

Citation for published version (Harvard):
Wasik, AM, Gandy, MN, McIldowie, M, Holder, M, Chamba, A, Challa, A, Lewis, KD, Young, S, Scheel-Toellner, D, Dyer, MJ, Gordon, J, Barnes, N & Piggott, MJ 2011, 'Enhancing the anti-lymphoma potential of 3,4-methylenedioxymethamphetamine ('ecstasy') through iterative chemical redesign: mechanisms and pathways to cell death', Investigational New Drugs. https://doi.org/10.1007/s10637-011-9730-5

Editorial Manager(tm) for Investigational New Drugs
Manuscript Draft

Manuscript Number:

Title: Enhancing the anti-lymphoma potential of 3,4-methylenedioxymethamphetamine ('ecstasy') through iterative chemical redesign: mechanisms and pathways to cell death

Article Type: Preclinical Trials

Keywords: Apoptosis; Bcl-2; Cytotoxicity; Lymphoma; MDMA

Corresponding Author: John Gordon, Ph.D.

Corresponding Author's Institution: University of Birmingham

First Author: Agata M Wasik, Ph.D.

Order of Authors: Agata M Wasik, Ph.D.;Michael N Gandy;Matthew McIldowie;Michelle J Holder;Anita Chamba;Anita Challa;Katie D Lewis;Stephen P Young;Dagmar Scheel-Toellner;Martin J Dyer;Nicholas M Barnes;Matthew J Piggott;John Gordon, Ph.D.

Enhancing the anti-lymphoma potential of 3,4-methylenedioxymethamphetamine ('ecstasy') through iterative chemical redesign: mechanisms and pathways to cell death

Agata M Wasik[1], Michael N Gandy[2], Matthew McIldowie[2], Michelle J Holder[1], Anita Chamba[1], Anita Challa[1], Katie D Lewis[2], Stephen P Young[1], Dagmar Scheel-Toellner[1], Martin J Dyer[3], Nicholas M Barnes[4], Matthew J Piggott[2], & John Gordon*[1]

(1) School of Immunity & Infection, The Medical School, Birmingham, UK

(2) School of Biomedical, Biomolecular and Chemical Sciences, The University of Western Australia, Crawley, Australia

(3) Medical Research Council Toxicology Unit, Leicester, UK.

(4) Cellular and Molecular Neuropharmacology Research Group, Clinical and Experimental Medicine, The Medical School, Birmingham, UK

*Corresponding author at: School of Immunity & Infection, The Medical School, Birmingham, University of Birmingham, Edgbaston, Birmingham B15 2TT UK.

Tel: +44 121 414 4034; fax: +44 121 414 3599. *E-mail address:* j.gordon@bham.ac.uk

Matthew J Piggott, Nicholas M Barnes, and John Gordon are joint senior authors

Summary

While 3,4-methylenedioxymethamphetamine (MDMA/'ecstasy') is cytostatic towards lymphoma cells *in vitro*, the concentrations required militate against its translation directly to a therapeutic *in vivo*. The possibility of 'redesigning the designer drug', separating desired anti-lymphoma activity from unwanted psychoactivity and neurotoxicity, was therefore mooted. From an initial analysis of MDMA analogues synthesized with a modified α-substituent, it was found that incorporating a phenyl group increased potency against sensitive, Bcl-2-deplete, Burkitt's lymphoma (BL) cells 10-fold relative to MDMA. From this lead, related analogs were synthesized with the 'best' compounds (containing 1- and 2-naphthyl and *para*-biphenyl substituents) some 100-fold more potent than MDMA *versus* the BL target. When assessed against derived lines from a diversity of B-cell tumors MDMA analogues were seen to impact the broad spectrum of malignancy. Expressing a *BCL2* transgene in BL cells afforded only scant protection against the analogues and across the malignancies no significant correlation between constitutive Bcl-2 levels and sensitivity to compounds was observed. Bcl-2-deplete cells displayed hallmarks of apoptotic death in response to the analogues while *bcl*-2-overexpressing equivalents died in a caspase-3-independent manner. Despite lymphoma cells expressing monoamine transporters, their pharmacological blockade failed to reverse the anti-lymphoma actions of the analogues studied. Neither did reactive oxygen species account for ensuing cell death. Enhanced cytotoxic performance did however track with predicted lipophilicity amongst the designed compounds. In conclusion, MDMA analogues have been discovered with enhanced cytotoxic efficacy against lymphoma subtypes amongst which high-level Bcl-2 – often a barrier to drug performance for this indication – fails to protect.

Keywords Apoptosis – Bcl-2 – Cytotoxicity – Lymphoma – MDMA

Abbreviations

ABC	Activated B-Cell-like
BL	Burkitt's lymphoma
DAT	Dopamine transporter
DLBCL	Diffuse large B-cell lymphoma
EBV	Epstein-Barr virus
FL	Follicular lymphoma
GCB	Germinal B-Cell-like
MDMA	3,4-methylenedioxymethamphetamine
NHL	Non-Hodgkin lymphomas
PARP	Poly (ADP-ribose) polymerase
PI	Propidium iodide
PTLD	Post-transplant lymphoproliferative disease
SERT	Serotonin transporter

Introduction

The incidence of B-cell lymphomas, constituting around 95% of all the non-Hodgkin lymphomas (NHL), is increasing steadily year-on-year. NHL is a heterogeneous group of neoplasia ranging from indolent examples like slow growing follicular lymphoma (FL) to highly aggressive, rapidly proliferating entities exemplified by diffuse large B-cell lymphoma (DLBCL) - the most common of the NHL in Europe, Australasia and the US - and Burkitt's lymphoma (BL): rare in the West but endemic in the World's malarial belt. The diversity of tumors reflects a composite of factors including the differentiation stage of the target B-cell and the mutations/translocations arising therein. Multiple profiling platforms such as gene array are disclosing additional heterogeneity within previously considered single clinical entities which can be manifested molecularly, cellularly and prognostically. DLBCL for example is now considered a composite of disease subtypes comprising primarily 'Activated B-Cell-like' (ABC) cases and those that are 'Germinal B-Cell-like' (GCB): survival rates among the former being substantially worse than the latter. Moreover, within ABC DLBCL constitutive expression of the pro-survival gene *BCL2* further discriminates a substantially inferior subgroup with regards overall survival even in the face of intense therapy.

Anti-apoptotic *BCL2*, originally identified as the gene translocating to the *IGH* locus on chromosome 14 in the hallmark t(14;18) of FL, offers a considerable barrier to drug efficacy in lymphoma treatment. BL, while extremely aggressive, lacks genetic alterations in *BCL2*, is deplete in Bcl-2 protein and has a high cure rate using combination chemotherapy. Over the past decade we have adopted BL as a template on which to explore novel therapeutic opportunities for lymphoma: BL offering a sensitive monitor of pro-apoptotic/anti-proliferative activities and at the same time being a tumor that is readily adaptable to tissue culture with derived lines remaining 'biopsy-like' when maintained in early passage. Transfection of

BCL2 on a constitutive promoter into these cells allows the opportunity to model directly on an otherwise isogenic background the impact of its dysregulated, high level expression on the efficacy of promising new drug candidates. Within this context we have been investigating compounds which target components of neurotransmitter pathways that can be found in immune cells and their cancers: most notably the transporters for serotonin and dopamine (SERT and DAT, respectively), each expressed in a broad range of the NHL subtypes and other B-cell malignancies [1-5].

Amongst such compounds, the amphetamine derivatives fenfluramine and 3,4-methylenedioxymethamphetamine (MDMA, 'Ecstasy') were found to be anti-proliferative against B-cell lines of diverse malignant B-cell origin. It was shown (at least with fenfluramine) that in Bcl-2-deplete BL cells, growth arrest was accompanied by apoptotic cell death following activation of caspase-3: these latter features being reversed on introducing *BCL2* as a transgene [4]. Unfortunately the concentrations of the amphetamine derivatives required to elicit anti-proliferative/pro-apoptotic activity *in vitro* were too high for safe translation to a cancer therapeutic *in vivo*. Therefore we mooted for MDMA the potential of "redesigning the designer drug" to enhance lymphoma killing while reducing neurotoxicity and psychoactivity.

Research by Shulgin and co-workers [6-9] suggests that extending the α- or *N*-substituent of MDMA to anything larger than an ethyl group abolishes the drug's psychoactivity. Nash and Nichols, studying acute effects in rats, showed that a simple substitution of the methyl group at the α-C of MDMA with an ethyl substituent, creating MBDB, significantly diminishes the amount of dopamine released in the striatum [10]. The α-substituent was therefore deemed a rational plinth for redesign. We now describe improved cytotoxic performance of MDMA

analogues with modified α-substituents against a spectrum of B-cell malignancies giving attention to the mechanisms and pathways to cell death, including the impact of anti-apoptotic Bcl-2. A companion study details in full the chemistry and synthesis of the analogues while providing evidence for diminished neurotoxicity and psychoactivity of selected compounds, together with a brief description of their rank potency in targeting a BL cell line [11].

Materials and Methods

Compounds

MDMA and analogues with modified α-substituents were synthesized by reductive amination of the corresponding piperonyl ketones as described recently [11]. All target amines were converted to their hydrochlorides and were tested as such.

Cell culture

Cell lines deriving from different B-cell malignancies and variants of the L3055 BL cell line were as described previously [4]. EBV-transformed lymphoblastoid cell lines were from the School of Cancer Sciences, University of Birmingham U.K. All cell lines were cultured in RPMI 1640 medium supplemented with 2mM glutamine, 10% v/v FCS, 100 U/ml penicillin, 100 U/ml streptomycin under 5% CO_2 at 37°C and passaged three times weekly.

Cellular cytotoxicity

Cellular cytotoxicity/viability was assessed by staining treated cells with propidium iodide (PI, a DNA binding dye incapable of penetrating intact cell membranes, (Sigma Aldrich, Dorset, UK)) at a final concentration of 0.85 µg/ml or 1.15 µg/ml prior to flow cytometric analysis

(FACS Calibur BD) of PI^{+ve} versus PI^{-ve} cells. Results were analysed using FlowJo 8 software for Macintosh.

Apoptosis

Apoptosis was assessed by dual staining of cells with PI and PhiPhiLux (Oncoimmunin, Gaithersburg, MD, USA) an indicator of active caspase-3 followed by analysis on FACS exactly as described previously [4]. Activation of caspase-3 was additionally assessed by staining cells with a rabbit antibody specific for the active form of caspase-3 (BD Pharmigen, Oxford, UK), followed by FACS analysis; non-immune rabbit IgG (control) was from Sigma Aldrich. Cells were pre-treated using the FIX and PERM kit for intracellular staining (Caltag, Invitrogen, Paisley, UK) according to the manufacturer's instructions. Cleavage of poly(ADP-ribose) polymerase-1 (PARP-1) as determined by Western blot and mitochondrial membrane permeability as assessed by JC-1 staining were performed as detailed elsewhere [3]. Bcl-2 protein content of cells was determined by Western blot as described previously [3].

Treatment with antioxidants

Cells were pre-treated with catalase (Sigma Aldrich, Dorset, UK) for 1 h or PEG-catalase (Sigma Aldrich, Dorset, UK) for 1.5 h before seeding cells onto 96-well plates containing MDMA/MDMA analogue. Cells at final density at 10^5/ml were incubated with drug for 24 h and cell viability was assessed by PI uptake analysed by flow cytometry.

Lipophilicity calculations

Estimates of lipophilicity were obtained from the "average log P" value output by the applet ALOGPs 2.1 available online [12]. A plot of average log P versus pIC_{50} showing the SEM in

each variable was constructed and a curve was fitted by weighted linear regression using Grafit 4, where the weighting of each point was inversely proportional to the respective error in pIC_{50}. Due to the uniformity in the magnitude of errors of average log P across the dataset, these were ignored when the weighted curve was fitted.

Pharmacological interpretation and statistics

Pharmacological interpretation of cytotoxicty assays to generate the pIC_{50} and Hill coefficient of a compound's activity against L3055 cells was performed using a four parameter logistic equation with iterative fitting using Kaleida Graph [13]. Regression analysis for cytotoxic response *vs* Bcl-2 expression was calculated as a ratio between remaining cell viability (assessed as in 2.3 above) following treatment with MDMA and analogues and the optical density (computed using ImageJ for Macintosh) of Bcl-2 *vs* calnexin protein bands as determined by Western blot. Graphs were created in OriginPro 8 (OriginLab, Northampton, MA).

Results

Substitutions at the α-carbon in MDMA can augment cytotoxic performance against L3055 Burkitt's lymphoma cells

The first generation of α-substituted MDMA analogues (Fig. 1a) synthesized contain either novel alkyl/cycloalkyl groups (compounds **1-5**) or, in the case of compound **6**, a phenyl substituent (structures presented in Fig. 1b). When assessed for anti-lymphoma potential against L3055, a prototype early-passage BL cell line, compound **6** was the most potent (approximately 10-fold>MDMA) both in inhibiting ^{3}H-thymidine incorporation (data not shown) and in its cytotoxic efficacy (Fig. 1c): $pIC_{50} = 4.12 \pm 0.03$ *versus* $pIC_{50} = 3.39 \pm 0.09$

for MDMA (Fig. 1b-c). Compound **6** therefore formed the template on which to design the next generation of compounds in the quest for a lymphoma therapeutic based on MDMA.

Larger aromatic α-substituents enhance cytotoxic potential towards L3055 cells

The second generation of α-modified MDMA analogues all contain aromatic rings (two in the case of compounds **16**, **17**, **18**), apart from compound **7**, which possesses a cyclohexyl group (Fig. 2a). The substituents in this series of MDMA analogues differ from each other with respect to three-dimensional structure, rigidity, and electron density: the benzene ring possessing all six carbons within one plane (sp^2-hybridized) by contrast to the cyclohexyl group, where the carbon atoms are sp^3-hybridized and therefore non-planar and conformationally flexible. Compound **8** has an α-benzyl group and thus an additional sp^3-hybridized carbon between the main carbon chain and the aromatic α-substituent. This provides additional flexibility compared to phenyl substituents, and extends the aromatic ring from the main chain, exploring the depth of a putative hydrophobic pocket in the target receptor(s).

Compounds **9**, **10** and **11** are more polar than their parent (**6**) due to the addition of a methoxy group. The lone pairs of electrons make the methoxy oxygens hydrogen bond acceptors, and also increase the electron density in the aromatic ring. Compounds **9**-**11** differ only in the position of the methoxy group. Similarly, compounds **13**, **14** and **15** possess *ortho*-, *meta*-, and *para*-methyl groups, respectively, exploring steric tolerance within the binding site(s). The *ortho*-substituents in **9** and **13** are also likely to reduce the range of low energy conformations available to the side chain.

Compound **12** contains fluorine in the *para*-position which reduces electron density in the aromatic ring but otherwise is very similar to a hydrogen atom (i.e. an isosteric replacement). Although the fluorine atom has three lone pairs of electrons, it is a very poor hydrogen bond acceptor and therefore adds to the hydrophobicity of the molecule [14,15]. Metabolic stability is also increased by the inclusion of fluorine.

Compounds **16**, **17** and **18** have much larger hydrophobic substituents at the α-position of MDMA, and therefore increased lipophilicity. The naphthyl group (compounds **16** and **17**) is highly rigid as all the carbon atoms are positioned in one plane, whereas the biphenyl group differs from compound 6 by the addition of a *para*-phenyl group and therefore both of the benzene rings are able to rotate around the axis of the bond between them.

From results presented in Fig. 2a-b it can be noted that from the second generation of MDMA analogues modified at the α-carbon, compounds **16**-**18** were by far the most potent regards cytotoxicity towards L3055 cells; compounds **17** and **18** being the most efficacious and equipotent with a pIC_{50} = 5.18±0.03 and 5.22±0.08; representing a ~10-fold and ~100-fold improvement over compound **6** and MDMA respectively. Similar rank potency of these analogues was observed when assessed for their capacity to inhibit ^{3}H-thymidine incorporation into L3055 cells (data not shown). It should be noted that all compounds tested for concentration-dependent cytotoxicity generated steep response curves yielding relatively high Hill coefficients (Fig. 1-2) suggesting deviation from simple mass interaction [16].

Cytotoxic efficacy of selected α-substituted MDMA analogues towards B-cell lines of different malignant derivation

The constituent cells of B-cell lines from a diverse range of malignancies were treated with MDMA and six of the α-substituted MDMA analogues (selected according to their activity versus sensitive L3055 cells and applied at a concentration at or close to their maximal cytotoxic performance against this cell line) then analysed for remaining viability (Fig. 3a). Given the resistance often afforded to therapeutic regimens by dysregulated/overexpressed *BCL2* in B-cell lymphoma, cells were simultaneously assessed for Bcl-2 protein content (*vs* calnexin standard) by Western blotting. The origin of cells spanned patients additional to those diagnosed with BL (L3055 series; KHM2B): precursor acute lymphoblastic leukemia (LILA), pro-lymphocytic leukemia (JVM2), mantle cell lymphoma (Rec-1; NCEB-1), primary mediastinal B-cell lymphoma (K1106), diffuse large B-cell lymphoma (K422; DoHH2), multiple myeloma (KMS11; H929). Immortalized B-cell lines generated from the peripheral blood of three donors by transformation with Epstein-Barr virus (EBV) were also included (HCD1; AT-AY; ViWo) – EBV being invariably linked to endemic BL, PTLD (post-transplant lymphoproliferative disease) and a high proportion of HIV-associated lymphoma.

MDMA and its analogues were set at concentrations displaying maximal/near-maximal impact on L3055 cell viability to serve as a reference. At these concentrations each of the analogues tested displayed (albeit a varying degree of) cytotoxicity against the spectrum of malignancies included. The best compound (**18**) showed a consistently substantive impact against each of the subtypes. As reported previously [4], Bcl-2 content showed some degree of correlation with a cell's ability to resist killing from MDMA. With each of the analogues, however, there was scant correlation between Bcl-2 protein level and extent of cytotoxicity observed (Fig. 3a). To assess the influence of Bcl-2 directly, a detailed concentration-dependent response was established for the cytotoxic efficacy of the analogues against L3055 cells transfected with empty vector versus cells expressing the *BCL2* transgene. The

latter were only marginally more resistant (approximately a single $\log_2$ difference) to each of the analogues than cells negative for Bcl-2 expression (Fig. 3b). This was consistent for cells plated at relatively low or high starting density.

Mode of cell death induced by selected first and second generation α-substituted MDMA analogues

When assessing cell integrity in response to compound **6** at 500 μM and compound 18 at 31.25 μM by dual PhiPhiLux (primarily detecting active caspase-3) and propidium iodide (plasma membrane permeability) staining, L3055 BL cells transfected with empty vector showed classic progression from early to late apoptosis over the course of the 6 hours monitored (Fig. 4a). While at the fixed concentration of the analogues used L3055-Bcl-2 cells again showed a degree of resistance to their cytotoxic actions, nevertheless the death that occurred failed to register an 'early apoptosis' stage at any time point as indicated by cells staining as PhiPhiLux+/PI-. While no PhiPhiLux positivity was developed with compound **6**, compound **18** progressively moved a portion of cells to what is conventionally considered a 'late apoptotic' stage: PhiPhiLux+/PI+. However, assessing engagement of the apoptotic machinery by alternative more direct methods gave no evidence for compound **18** provoking this pathway in L3055-Bcl-2 cells. Thus the specific detection of active caspase-3 by antibody revealed its appearance in response to compounds **6** and **18** in L3055-VC but not in L3055-Bcl-2 cells (Fig. 4b). Likewise, the cleavage of poly (ADP-ribose) polymerase (PARP) [17], as shown occurring in L3055-VC cells with the well characterized apoptosis-inducing agent anti-IgM, was also seen on application of MDMA and here more potently with compounds **16**, **17**, and **18** whereas L3055-Bcl-2 cells revealed little if any PARP cleavage in response to any of the agents applied (Fig. 4c). JC-1 staining to indicate collapse of

mitochondrial potential [1] similarly supported the different routes to cell death by analogs depending on the expression of Bcl-2 in L3055 BL cells (data not shown).

Mechanisms and pathways to lymphoma cell killing by selected α-substituted MDMA analogues

Depending upon cell type and system studied, MDMA has been purported to provoke toxicity via a diverse array of not necessarily mutually exclusive pathways as reviewed for example in [18]. Here, the possible involvement of monoamine transporters in delivering MDMA and its analogues to engage intracellular pathways for lymphoma B-cell killing was first investigated. For this, L3055-VC cells were pre-treated with a range of monoamine transporter (MAT) inhibitors targeting: SERT (fluoxetine), SERT and NET (clomipramine and imipramine) or DAT (GBR12909); and also with cocaine, which blocks all three MATs. From results detailed in Fig. 5a it can be seen that none of the MAT inhibitors afforded protection against lymphoma cell toxicity induced by MDMA or two of its more potent analogues indicating that they are unlikely to be serving as conduits to the compounds' actions in this regard.

Since MDMA has been widely reported to mediate toxicity via direct or indirect production of reactive oxygen species (ROS), L3055-WT and -VC cells were pre-treated with enzymes that either degrade superoxide ($O_2^{\bullet -}$) (superoxide dismutase, SOD) or H_2O_2 (catalase). However, neither SOD (data not detailed) nor catalase were seen to protect tumor B cells from the detrimental effect of the MDMA analogues studied, whereas catalase efficiently reversed cell killing provoked by H_2O_2 (Fig. 5b). Cells pre-treated with these enzymes but now conjugated to polyethylene glycol (PEG) to facilitate cell uptake [19,20] similarly failed to protect (Fig. 5c and data not detailed).

Finally, we examined the possibility that increased lipophilicity may be associated with the enhanced anti-lymphoma performance of the more potent analogues in this study. To explore this, we used the online program, ALOGPs 2.1, which accepts a structural formula to generate an estimate of lipophilicity where the output value is known as “average log P” [21]. In brief, the average log P value is the simple average of log P estimates determined using eight different models. A plot of average log P versus the pIC_{50} value of cytotoxic performance (including SEM values for both variables) was constructed and a curve was fitted by weighted linear regression as detailed in Fig. 6. When operating at pH values that favour ionisation of the compounds under consideration, as in this case (pH=7.4), log P values should be corrected using the pK_a to account for the increase in aqueous solubility of the ionised form. However, uncorrected log P values were used here as the pK_a values (dictated by the shared amino group), and therefore the correction factors, were expected to be very similar for all compounds, thus, not affecting the rank order obtained. Furthermore, the use of uncorrected log P predictions to estimate lipophilicity has been shown to be more reliable, as it avoids the introduction of a second source of error associated with the calculation of pK_a [22]. Bearing these considerations in mind, a persuasive correlation emerges with $r^2 = 0.88$ as seen in Fig. 6.

Discussion

Analogues of MDMA with modified α-substituents were iteratively designed and synthesised, and found to be up to 10-fold (first generation) and 100-fold (second generation) more potent than the parent amphetamine derivative at promoting lymphoma cell death: the goal and driver to this study. Impressively, forced over-expression or high constitutive levels of anti-apoptotic Bcl-2 failed to protect, to any significant degree, the anti-lymphoma actions of

the analogues; this despite their ability to promote apoptotic cell death in Bcl-2-deplete cells. Thus, in the face of high-level Bcl-2, death still occurred but in a caspase-3-, PARP-independent fashion that was similarly independent from a collapse in mitochondrial membrane potential. It should be noted, however, that while analogues of MDMA efficiently generated active caspase-3 within 4-6 hours of exposure in the bulk of native L3055 BL cells, a majority of their Bcl-2-overexpressing counterparts were still alive at 6 hours. Thus, at least for BL, if translated to an *in vivo* therapeutic, these compounds show potential to reduce tumor burden through efficient apoptotic clearance without the attendant inflammatory side effects of necrotic death.

Importantly, improved cytotoxic performance against lymphoma cells does not simply reflect a generally enhanced, non-specific toxicity profile of the compounds. A companion study shows that the most active compound *versus* lymphoma cells from Series 1 (compound **6**) and two of the even more active ones from Series 2 (compounds **16** and **17**) are in fact less toxic than MDMA to SH-SY5Y: a catecholaminergic neuroblastoma cell line that is used to model MDMA neurotoxicity. The same study also shows compound 6 having diminished psychoactivity when compared with MDMA in the prepulse inhibition of the acoustic startle reflex test in Wistar rats [11]. Furthermore, in the present study, while constituent cells of derived lines from all B-cell malignancies proved susceptible to one or more of the analogues tested, the relative level of sensitivity to a given compound could be quite different depending upon the cell line targeted indicating a degree of selectivity in the compounds' actions against lymphoma cell subtypes.

The literature around MDMA and the mechanisms underlying its toxicity is large, varied and occasionally contradictory [23-31]: the cell system, cellular origin, animal species, drug

concentration and other elements all contributing confounding factors. Here we scrutinized several of the major candidate pathways proposed for MDMA for their potential contribution to the toxic action of the analogues *versus* B-lymphoma cells. The current study was predicated on the discovery that B lymphoma cells express both SERT and DAT, the transporters for serotonin and dopamine, respectively, and to which MDMA binds in the human with high affinity as it also does to NET, the norepinephrine transporter [32,30]. Against serotonergic JAR cells for example, MDMA's cytotoxicity is delivered via SERT: being inhibited by imipramine, a monoamine transporter blocker with highest affinity for SERT [33]. The capacity of serotonin to drive apoptosis in BL cells is reversed by SERT blockade with e.g. the selective serotonin reuptake inhibitor, fluoxetine [1]. However, adopting the approach of pharmacological transporter blockade in this work, neither MDMA nor two of its more potent redesigned analogues were seen to be delivering their toxic hit to lymphoma cells via any of the three monoamine transporters probed. Moreover, Montgomery and colleagues [34] examining the action of MDMA and several MDMA analogues on 5-HT and NA uptake in cells transfected with SERT or NET reported a Hill coefficient for inhibition by MBDB (our compound **3**) of ~1 for both HEK-SERT and PC12-NET compared to that generated from its anti-lymphoma action in this study of >3. Others have shown that MDMA is capable of promoting cell death independently of SERT expression or activity [35]. A second major mechanism for MDMA's cellular toxicity in other systems was similarly ruled out here for both the lead compound and the more (anti-lymphoma) potent synthesized analogues: namely the, direct or indirect, production of reactive oxygen species. Inhibitors of extracellular ROS which have previously been shown to reverse the anti-lymphoma actions of dopamine [36] did not protect against MDMA and its analogues in this respect. Similar failure of PEGylated SOD and catalase to inhibit death

delivered from the compounds under study equally argued against intracellular ROS formation contributing to the lymphoma cell killing observed.

If not through ROS generation or from entering via monoamine transporters, how are MDMA and its redesigned analogues attacking the lymphoma cells? Screening against the sensitive L3055 cell line revealed no significant difference in the cells' response to compounds containing α-subsituents with either different steric (**13**-**15**, **16**-**17**) or stereoelectronic (**9**-**12**) properties. Instead, the addition of further aromatic rings, thereby increasing the size of substituents at the α-carbon of MDMA, appeared a unifying factor to increasing potency: i.e. compound **6** in Series 1 with a single aromatic ring and compounds **18**, **17** and **16** in Series 2 with two aromatic rings being the most potent from each iteration. That said, the non-aromatic cyclohexyl substituent confers equipotency to phenyl. Size of the α-subsituent and overall lipophilicity of the compound may therefore be primary determinants of potency. In an earlier study we noted from a seemingly otherwise disparate set of compounds capable of killing lymphoma cells the shared feature of being cationic amphiphiles [4]. This class of compounds has the capacity to disrupt cellular membranes, as do amphiphilic molecules generally. Greater lipophilicity also enhances entry into cells, thereby increasing the effective intracellular concentration, and entropically favours complex formation (the hydrophobic effect) and thus, potentially, affinity of drug for intracellular receptors/targets. Numerous studies indicate a selectivity of lipophilic compounds for impacting rapidly proliferating cancer cells over normal cells [37,38] and others show, amongst related series of compounds, a clear correlation between anti-proliferative activity/cytotoxicity and degree of lipophilicity [39-41]. When this relationship was examined for the newly synthesized analogues of MDMA, a strong correlation was indeed observed with anti-lymphoma potency closely tracking calculated lipophilicity, at least for those compounds with aromatic α-

substituents. We are currently exploring precisely how this physiochemical property of the compounds translates mechanistically to improved lymphoma killing in order to assist further rational design of MDMA analogues as anti-neoplastics.

Irrespective of relative anti-lymphoma potency all compounds including MDMA generated steep inhibition curves with Hill coefficients >3 indicating a high degree of cooperativity in their action. Similar behaviour has been observed from SSRIs and tricyclic antidepressants (Serafeim Blood 2003; Meredith FASEB J 2005) and at least with the former class of compound we know that cell death is preceded by the stimulation of Ca^{2+} entry. Preliminary data (unpublished) indicate similarly altered Ca^{2+} flux in L3055 BL cells on exposure to MDMA and analogues studied here. As an alternative to cooperative binding at a defined molecular target, a possibility under consideration is that the lipophilic compounds undergo aggregate formation dependent upon a critical association concentration – perhaps established *in situ* within the lipid bilayer of the cell membrane [42] – and that it is these higher order complexes that cause cell death conceivably analogous to – or directly behaving as – ionophores [43].

In conclusion, a series of iterations positioned on a modified α-substituent of MDMA resulted in a number of lead compounds with respect to prospective novel therapeutics for non-Hodgkin lymphomas. Insight into the mechanism of their actions and the pathways by which they promote cell death opens a door to further rational modifications that hold the promise of accelerating translation of a redesigned MDMA to the clinic for this important cancer indication.

Acknowledgements

This work was supported in part by Leukaemia and Lymphoma Research, UK, and the Ada Bartholomew Medical Research Trust, W.A. MNG and KDL were recipients of a UWA postgraduate scholarship and Australian Postgraduate Award, respectively. DS-T was supported by an Arthritis Research UK Career Progression Fellowship. JG was in receipt of a Raine Visiting Professorship at the University of Western Australia while writing the paper. The authors declare that they have no conflict of interest.

References

1. Serafeim A, Grafton G, Chamba A, Gregory CD, Blakely RD, Bowery NG, Barnes NM, Gordon J (2002) 5-Hydroxytryptamine drives apoptosis in biopsylike Burkitt lymphoma cells: reversal by selective serotonin reuptake inhibitors. Blood 99:2545-2553

2. Meredith EJ, Chamba A, Holder MJ, Barnes NM, Gordon J (2005) Close encounters of the monoamine kind: immune cells betray their nervous disposition. Immunology 115:289-295

3. Serafeim A, Holder MJ, Grafton G, Chamba A, Drayson MT, Luong QT, Bunce CM, Gregory CD, Barnes NM, Gordon J (2003) Selective serotonin reuptake inhibitors directly signal for apoptosis in biopsy-like Burkitt lymphoma cells. Blood 101:3212-3219

4. Meredith EJ, Holder MJ, Chamba A, Challa A, Drake-Lee A, Bunce CM, Drayson MT, Pilkington G, Blakely RD, Dyer MJ, Barnes NM, Gordon J (2005) The serotonin transporter (SLC6A4) is present in B-cell clones of diverse malignant origin: probing a potential anti-tumor target for psychotropics. FASEB J 19:1187-1189

5. Chamba A, Holder MJ, Jarrett RF, Shield L, Toellner KM, Drayson MT, Barnes NM, Gordon J SLC6A4 expression and anti-proliferative responses to serotonin transporter ligands chlomipramine and fluoxetine in primary B-cell malignancies. Leuk Res 34:1103-1106

6. Braun U, Shulgin AT, Braun G (1980) Centrally active N-substituted analogs of 3,4-methylenedioxyphenylisopropylamine (3,4-methylenedioxyamphetamine). J Pharm Sci 69:192-195

7. Braun U, Shulgin AT, Braun G (1980) [Research on the central activity and analgesia of N-substituted analogs of the amphetamine derivative 3,4-methylenedioxyphenylisopropylamine]. Arzneimittelforschung 30:825-830

8. Nichols DE, Hoffman AJ, Oberlender RA, Jacob P, 3rd, Shulgin AT (1986) Derivatives of 1-(1,3-benzodioxol-5-yl)-2-butanamine: representatives of a novel therapeutic class. J Med Chem 29:2009-2015
9. Shulgin A, Shulgin A (1991) Phenethylamines I Have Known And Loved: A Chemical Love Story Transform Pr Berkeley, California
10. Nash JF, Nichols DE (1991) Microdialysis studies on 3,4-methylenedioxyamphetamine and structurally related analogues. Eur J Pharmacol 200:53-58
11. Gandy MN, McIldowie M, Lewis K, Wasik AM, Salomonczyk D, Wagg K, Millar ZA, Tindiglia D, Huot P, Johnston T, Thiele S, Nguyen B, Barnes NM, Brotchie JM, Martin-Inverson MT, Nash J, Gordon J, Piggott MJ (2010) Redesigning the designer drug ecstasy: non-psychoactive MDMA analogues exhibiting Burkitt's lymphoma cytotoxicity. Med Chem Comm 1:287-293
12. Tetko IV, Gasteiger J, Todeschini R, Mauri A, Livingstone D, Ertl P, Palyulin VA, Radchenko EV, Zefirov NS, Makarenko AS, Tanchuk VY, Prokopenko VV (2005) Virtual computational chemistry laboratory--design and description. J Comput Aided Mol Des 19:453-463
13. Steward LJ, Ge J, Bentley KR, Barber PC, Hope AG, Lambert JJ, Peters JA, Blackburn TP, Barnes NM (1995) Evidence that the atypical 5-HT3 receptor ligand, [3H]-BRL46470, labels additional 5-HT3 binding sites compared to [3H]-granisetron. Br J Pharmacol 116:1781-1788
14. Bohm HJ, Banner D, Bendels S, Kansy M, Kuhn B, Muller K, Obst-Sander U, Stahl M (2004) Fluorine in medicinal chemistry. Chembiochem 5:637-643
15. Smart BE (2001) Fluorine Substutuent Effects (on Bioactivity). J Fluorine Chem 109:3-11
16. Cornish-Bowden A, Koshland DE, Jr. (1975) Diagnostic uses of the Hill (Logit and Nernst) plots. J Mol Biol 95:201-212
17. Boulares AH, Yakovlev AG, Ivanova V, Stoica BA, Wang G, Iyer S, Smulson M (1999) Role of poly(ADP-ribose) polymerase (PARP) cleavage in apoptosis. Caspase 3-resistant PARP mutant increases rates of apoptosis in transfected cells. J Biol Chem 274:22932-22940
18. Cadet JL, Krasnova IN, Jayanthi S, Lyles J (2007) Neurotoxicity of substituted amphetamines: molecular and cellular mechanisms. Neurotox Res 11:183-202
19. Beckman JW, Wang Q, Guengerich FP (2008) Kinetic analysis of correct nucleotide insertion by a Y-family DNA polymerase reveals conformational changes both prior to and

following phosphodiester bond formation as detected by tryptophan fluorescence. J Biol Chem 283:36711-36723
20. Blatt NB, Boitano AE, Lyssiotis CA, Opipari AW, Jr., Glick GD (2009) Bz-423 superoxide signals B cell apoptosis via Mcl-1, Bak, and Bax. Biochem Pharmacol 78:966-973
21. Tetko IV, Tanchuk VY (2002) Application of associative neural networks for prediction of lipophilicity in ALOGPS 2.1 program. J Chem Inf Comput Sci 42:1136-1145
22. Tetko IV, Bruneau P (2004) Application of ALOGPS to predict 1-octanol/water distribution coefficients, logP, and logD, of AstraZeneca in-house database. J Pharm Sci 93:3103-3110
23. Yamamoto B, Zhu W (1998) The effects of methamphetamine on the production of free radicals and oxidative stress. . J Pharmacol Exp Ther 287:107-114
24. Davidson C, Gow A, Lee T, Ellinwood E (2001) Methamphetamine neurotoxicity: necrotic and apoptotic mechanisms and relevance to human abuse and treatment. Brain Res Brain Res Rev 36 (1):1-22
25. Yamamoto BK, Bankson MG (2005) Amphetamine neurotoxicity: cause and consequence of oxidative stress. Crit Rev Neurobiol 17:87-117
26. Montiel-Duarte C, Ansorena E, Lopez-Zabalza M, Cenarruzabeitia E, Iraburu M (2004) Role of reactive oxygen species, glutathione and NF-kappaB in apoptosis induced by 3,4-methylenedioxymethamphetamine ("Ecstasy") on hepatic stellate cells. . Biochem Pharmacol 67:1025-1033
27. Monks TJ, Jones DC, Bai F, Lau SS (2004) The role of metabolism in 3,4-(+)-methylenedioxyamphetamine and 3,4-(+)-methylenedioxymethamphetamine (ecstasy) toxicity. Ther Drug Monit 26:132-136
28. Milhazes N, Cunha-Oliveira T, Martins P, Garrido J, Oliveira C, Rego AC, Borges F (2006) Synthesis and cytotoxic profile of 3,4-methylenedioxymethamphetamine ("ecstasy") and its metabolites on undifferentiated PC12 cells: A putative structure-toxicity relationship. Chem Res Toxicol 19:1294-1304
29. Keizers PH, de Graaf C, de Kanter FJ, Oostenbrink C, Feenstra KA, Commandeur JN, Vermeulen NP (2005) Metabolic regio- and stereoselectivity of cytochrome P450 2D6 towards 3,4-methylenedioxy-N-alkylamphetamines: in silico predictions and experimental validation. J Med Chem 48:6117-6127
30. Capela JP, Carmo H, Remiao F, Bastos ML, Meisel A, Carvalho F (2009) Molecular and cellular mechanisms of ecstasy-induced neurotoxicity: an overview. Mol Neurobiol 39:210-271

31. Callahan BT, Cord BJ, Yuan J, McCann UD, Ricaurte GA (2001) Inhibitors of Na(+)/H(+) and Na(+)/Ca(2+) exchange potentiate methamphetamine-induced dopamine neurotoxicity: possible role of ionic dysregulation in methamphetamine neurotoxicity. J Neurochem 77:1348-1362
32. Verrico CD, Miller GM, Madras BK (2007) MDMA (Ecstasy) and human dopamine, norepinephrine, and serotonin transporters: implications for MDMA-induced neurotoxicity and treatment. Psychopharmacology (Berl) 189:489-503
33. Simantov R, Tauber M (1997) The abused drug MDMA (Ecstasy) induces programmed death of human serotonergic cells. FASEB J 11 (2):141-146
34. Montgomery T, Buon C, Eibauer S, Guiry PJ, Keenan AK, McBean GJ (2007) Comparative potencies of 3,4-methylenedioxymethamphetamine (MDMA) analogues as inhibitors of [3H]noradrenaline and [3H]5-HT transport in mammalian cell lines. Br J Pharmacol 152:1121-1130
35. Hayat S, Williams RJ, Rattray M (2006) Serotonin transporter expression is not sufficient to confer cytotoxicity to 3,4-methylenedioxymethamphetamine (MDMA) in vitro. J Psychopharmacol 20:257-263
36. Meredith EJ, Holder MJ, Rosen A, Lee AD, Dyer MJ, Barnes NM, Gordon J (2006) Dopamine targets cycling B cells independent of receptors/transporter for oxidative attack: Implications for non-Hodgkin's lymphoma. Proc Natl Acad Sci U S A 103 (36):13485-13490
37. Biasutto L, Dong LF, Zoratti M, Neuzil J Mitochondrially targeted anti-cancer agents. Mitochondrion 10:670-681
38. Christman JE, Miller DS, Coward P, Smith LH, Teng NN (1990) Study of the selective cytotoxic properties of cationic, lipophilic mitochondrial-specific compounds in gynecologic malignancies. Gynecol Oncol 39:72-79
39. Huszar M, Varga A, Horvath A, Lorand T, Agocs A, Idei M, Mandl J, Vantus T, Keri G Comparative characterization of experimental and calculated lipophilicity and anti-tumour activity of isochromanone derivatives. Curr Med Chem 17:321-333
40. Adams DJ, da Silva MW, Flowers JL, Kohlhagen G, Pommier Y, Colvin OM, Manikumar G, Wani MC (2006) Camptothecin analogs with enhanced activity against human breast cancer cells. I. Correlation of potency with lipophilicity and persistence in the cleavage complex. Cancer Chemother Pharmacol 57:135-144

41. Maliepaard M, de Mol NJ, Janssen LH, van der Neut W, Verboom W, Reinhoudt DN (1992) Role of lipophilicity in the in vitro antitumour activity of a series of new mitosene compounds. Anticancer Drug Des 7 (5):415-425
42. Soderberg L, Haag L, Hoglund P, Roth B, Stenberg P, Wahlgren M (2009) The effects of lipophilic substances on the shape of erythrocytes demonstrated by a new in vitro-method. Eur J Pharm Sci 36 (4-5):458-464
43. Sanderson KL, Butler L, Ingram VM (1997) Aggregates of a beta-amyloid peptide are required to induce calcium currents in neuron-like human teratocarcinoma cells: relation to Alzheimer's disease. Brain Res 744 (1):7-14

Figure captions

Fig 1 *Cytotoxic efficacy of MDMA and Series 1 (first generation) MDMA analogues versus L3055 Burkitt's lymphoma cells.* (a) Chemical structure of MDMA with α-carbon (α-C) indicated; (b) MDMA analogues with the first iteration of α-C substituents constituting Series 1 compounds **1**-**6** as shown, together with calculated pIC_{50} ± SEM and Hill coefficients ± SEM from response curves as generated in (c) with number of separate experiments performed with each compound given as 'n'; (c) typical concentration-response curves showing cytotoxic performance of MDMA and Series 1 analogues against the L3055 BL cell line. Cells were cultured at $5x10^5$/ml with MDMA or indicated analogue at concentrations shown for 48h prior to measuring cytotoxicity by PI uptake using flow cytometry. Results are represented as the mean of three independent experiments ± SEM in terms of the percentage of cells remaining viable with respect to vehicle (no drug) control

Fig 2 *Cytotoxic efficacy of Series 2 (second generation) analogues versus L3055 Burkitt's lymphoma cells.* (a) and (b) as for (b) and (c) respectively in Fig.1 but here with Series 2 compounds **7**-**18**; MDMA again included for comparison

Fig 3 *Cytotoxic performance of MDMA and selected analogues against B-cell lines of different malignant derivation and relationship to Bcl-2 expression.* (a) Cells from lines as shown plated at $5x10^5$/ml and cultured for 24h with compounds indicated prior to assessing (absolute) % viability of population as in Fig.1c. Concentration of drug applied as follows: MDMA, 2000 μM; compound **6**, 500 μM; compound **12**, 250 μM; compound **15**, 125 μM; compound **16**, 31.25 μM; compound **17**, 31.25 μM; compound **18**, 31.25 μM. Below is shown representative western blot analysis of Bcl-2 protein levels amongst the lines together with calnexin blotting control. Next are shown regression plots with R values

generated from remaining % viability in response to compound *versus* relative Bcl-2 content amongst the lines tested; (b) concentration response curves to compounds of L3055 cells carrying empty vector (L3055-VC) or a Bcl-2 transgene (L3055-Bcl2). Cells were plated at two different starting densities, 10^5 cells/ml and $5x10^5$ cells/ml as indicated, and incubated with compound for 24h prior to assessing viability/cytotoxicity as in Fig.1c. Results represent the mean of three independent experiments ± SEM given as % viability relative to vehicle control

Fig 4 *Mode of cell death in L3055-VC and L3055/Bcl2 cells in response to MDMA analogues **6** and **18**.* (a) Cells from L3055 variant lines indicated were cultured with compound **6** (500 µM) or compound **18** (31.25 µM) for 6h before dual staining with PhiPhiLux (PPL) and PI (upper graph; dot plots) revealing four subpopulations of cells: PI^{lo}/PPL^{lo} = viable (bottom left quadrant), PI^{lo}/PPL^{hi} = early apoptotic (bottom right), PI^{hi}/PPL^{hi} = late apoptotic (top right), and PI^{hi}/PPL^{hi} = necrotic (top left). The lower set of graphs illustrate similar analyses arising from exposing cells to the compounds over 1-6h with the data represented as the % of cells arising in each quadrant at the different times of harvest: viable marked in white, early apoptotic marked light grey, late apoptotic marked dark grey, necrotic marked black. Data are the mean of three independent experiments (n=3) ± SEM with the values shown obtained after subtracting vehicle control; (b) L3055-VC and L3055-Bcl2 cells at $5x10^5$/ml treated for 2h with compound **6** at 500µM and compound **18** at 31.25 µM (black line) or vehicle control (shaded) then stained with antibody to active caspase-3 with intensity of staining analysed by FACS. A representative example of two independent experiments is shown. (c) Western blot analysis of PARP cleavage in L3055-VC and L3055-Bcl2 cells plated at 10^6/ml and treated for 6h with MDMA at 2000 µM or compounds **16**, **17** or **18** at 31.25 µM; upper 117kDa band = intact PARP, lower 97kDa band = cleaved PARP; anti-IgM (25 µg/ml) is a positive control

treatment known to signal PARP cleavage in L3055-VC cells via cell surface BCR. This experiment was performed twice with a representative example shown

Fig 5 *Investigation of potential pathways through which MDMA analogues elicit cytotoxicity in L3055 cells.* (a) Impact of monoamine transporter (MAT) inhibitors. L3055 cells at 10^5/ml were pre-incubated with MAT inhibitors for 1h before adding MDMA or compounds **15** and **16** at 125 µM and 31.25 µM respectively then culturing for 20h prior to assessing cell viability as in Fig.1c; (b) Influence of scavenging extracellular ROS with catalase. L3055 cells at 10^5/ml were pre-treated with catalase at concentrations shown for 1h before adding H_2O_2 or compounds indicated (compound **6**, 500 µM; compound **12**, 250 µM; compound **15**, 125 µM; compounds **16**, **17** and **18**, 31.25 µM) and then culturing for 20h prior to assessing viability as above; (c) Influence of scavenging intracellular ROS with PEG-catalase. L3055-VC cells at 10^5/ml were pre-treated with PEG-catalase for 1.5h before adding H_2O_2, MDMA, or compound **6** at concentrations indicated and then culturing for 24h prior to assessing viability.

Fig 6 *Calculated liphophilicities of MDMA and analogues* versus *cytotoxic performance*. Relationship between average log P ± SEM and pIC_{50} ± SEM for MDMA (□), alkyl α-substituted analogues **1-5** (◇), monocyclic aromatic α-substituted analogues **6**-**15** (△) and polycyclic aromatic α-substituted analogues **16**-**18** (○). The curve was fitted to all data points shown using weighted linear regression that gave an r^2 value of 0.88

Figure 1

Click here to download Figure: Fig.1.ppt

a.

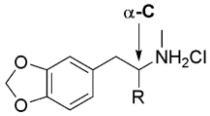

b.

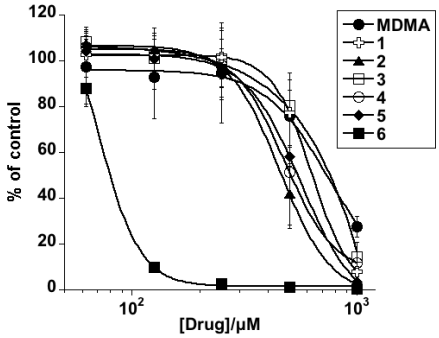

compound	α-substituent	pIC_{50} ± SEM	Hill coefficient ± SEM	n
MDMA		3.39 ± 0.09	3.89 ± 1.12	14
1		3.10 ± 0.02	3.33 ± 0.73	3
2		3.36 ± 0.06	4.56 ± 0.98	3
3		3.15 ± 0.01	3.4 ± 0.93	3
4		3.42 ± 0.03	4.79 ± 0.77	3
5		3.20 ± 0.07	3.40 ± 0.81	3
6		4.12 ± 0.03	4.65 ± 0.31	8

Figure 2

Click here to download Figure: Fig.2.ppt

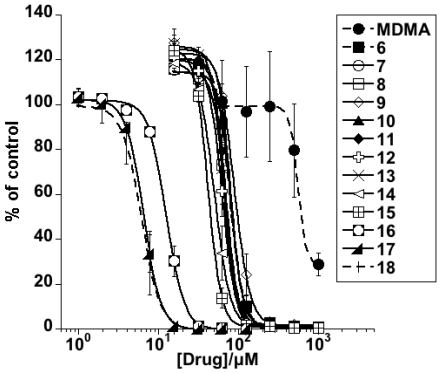

compound	α-substituent	pIC_{50} ± SEM	Hill coefficient ± SEM	n
7		4.10 ± 0.04	6.56 ± 0.43	3
8		4.16 ± 0.03	5.92 ± 0.58	3
9	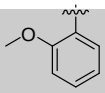	4.04 ± 0.04	4.82 ± 0.38	3
10	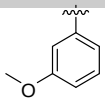	4.10 ± 0.01	6.05 ± 0.16	3
11	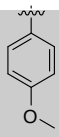	4.16 ± 0.02	5.60 ± 0.73	3
12	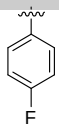	4.20 ± 0.02	5.89 ± 1.12	3
13		4.20 ± 0.05	6.68 ± 073	3
14	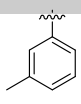	4.29 ± 0.05	5.05 ± 0.17	3
15	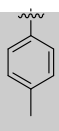	4.37 ± 0.03	5.69 ± 0.27	3
16	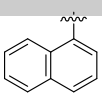	4.90 ± 0.02	4.04 ± 0.74	3
17	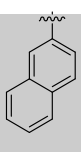	5.18 ± 0.03	4.38 ± 0.73	3
18	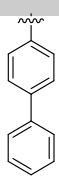	5.22 ± 0.08	5.05 ± 0.97	3

Figure 3

Click here to download Figure: Fig.3.ppt

a

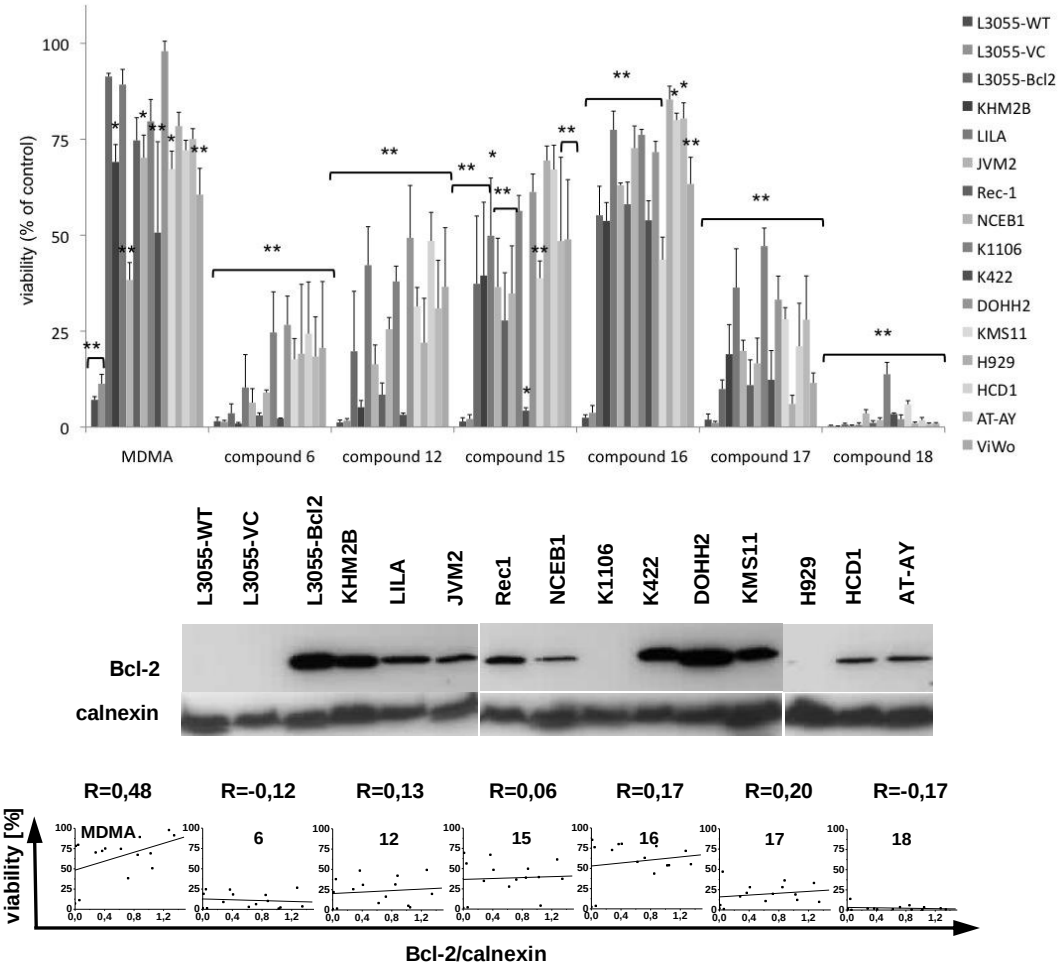

b.

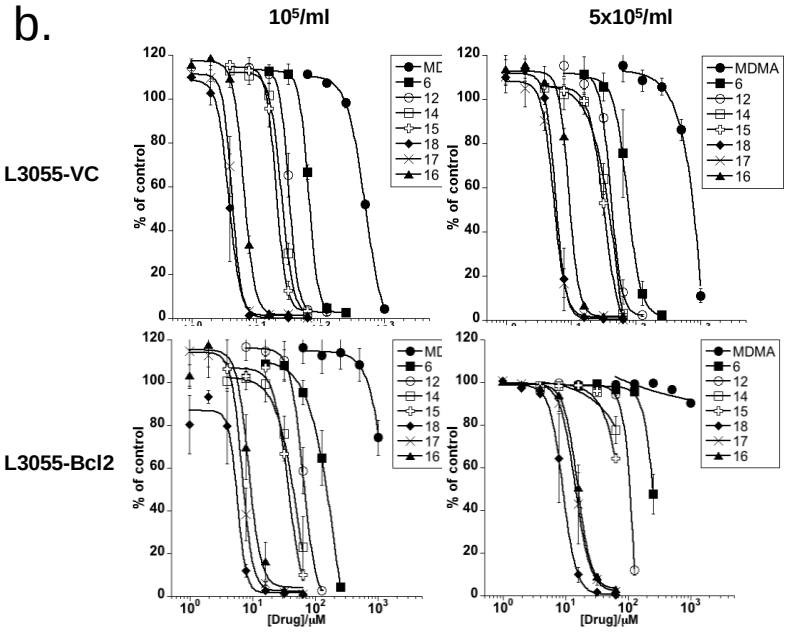

Figure 4

Click here to download Figure: Fig.4.ppt

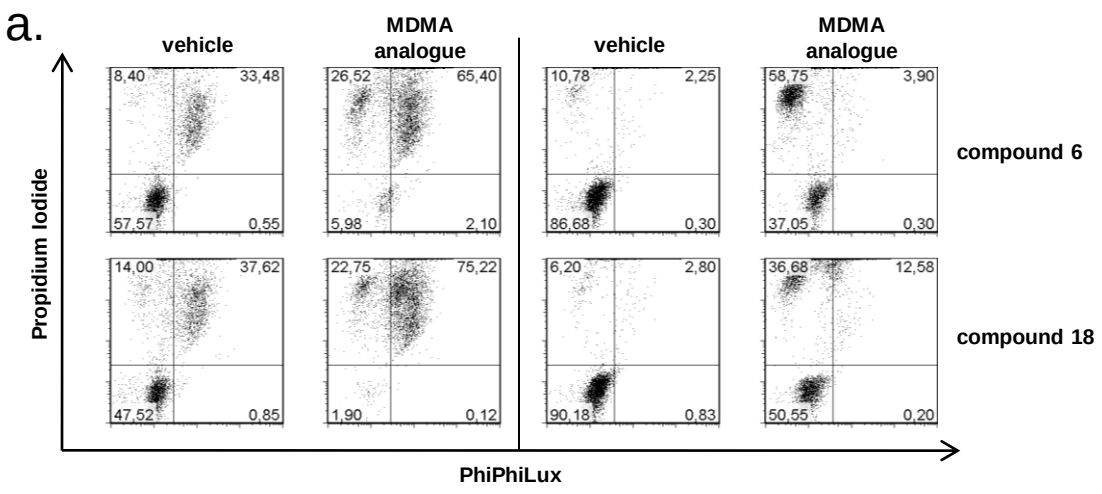

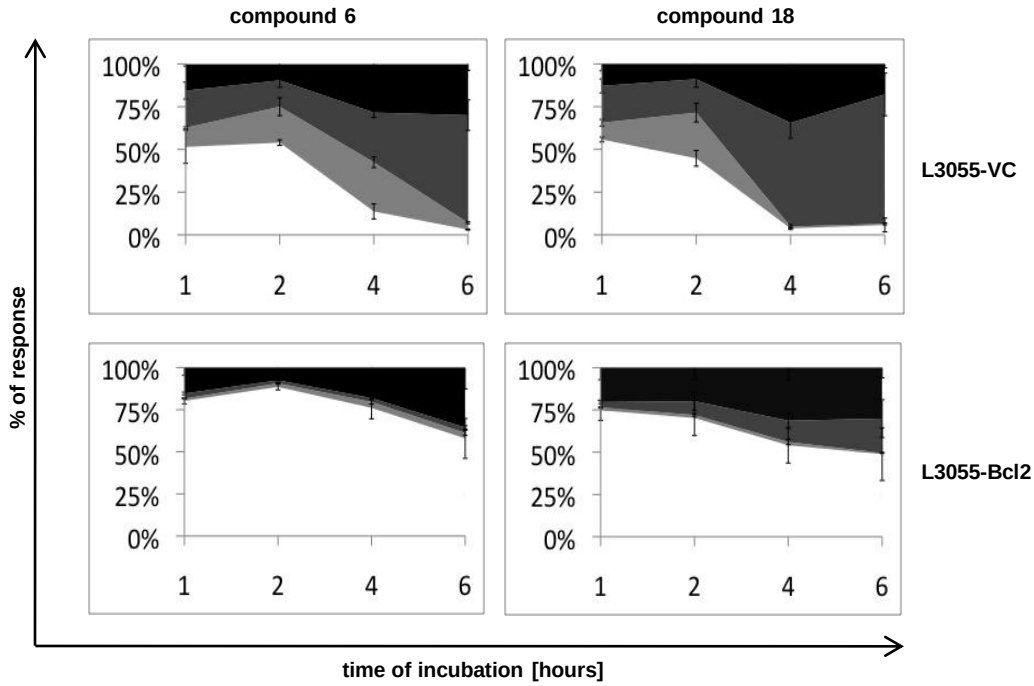

b.

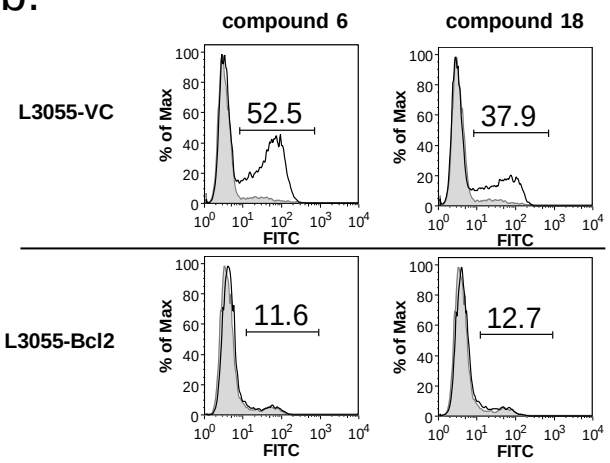

c.

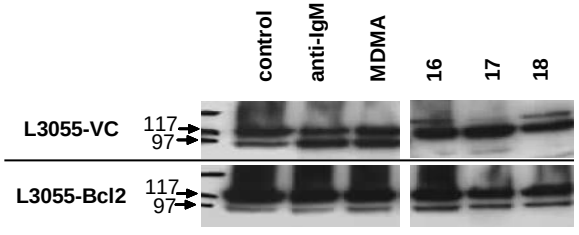

Figure 5

Click here to download Figure: Fig.5.ppt

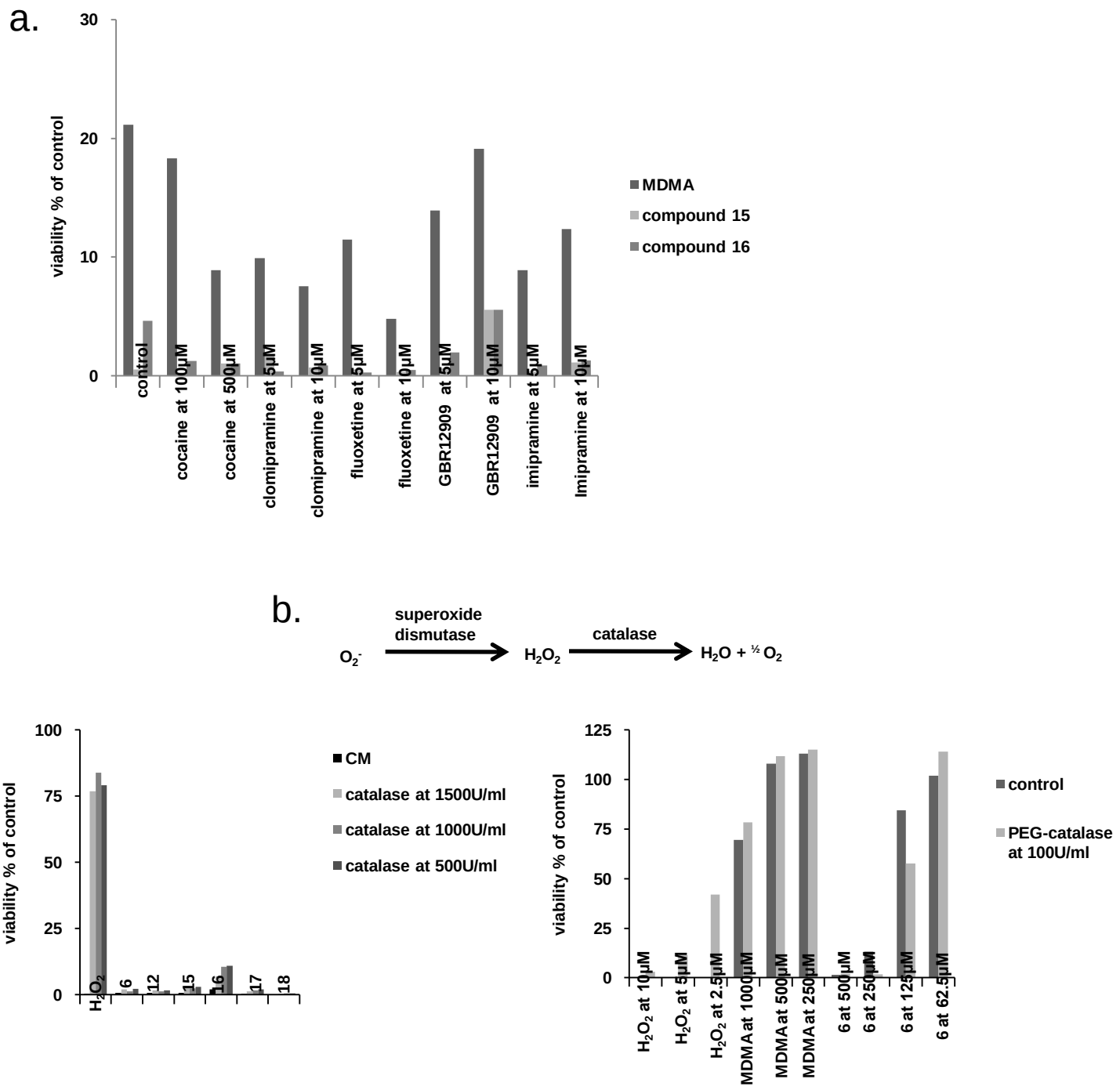

Figure 6

Click here to download Figure: Fig.6.ppt